Fully Automated Volumetric Breast Density Estimation from Digital Breast Tomosynthesis

Aimilia Gastounioti, PhD • Lauren Pantalone, MPH • Christopher G. Scott, MS • Eric A. Cohen, MS • Fang F. Wu, BS • Stacey J. Winham, PhD • Matthew R. Jensen, BS • Andrew D. A. Maidment, PhD • Celine M. Vachon, PhD • Emily F. Conant, MD • Despina Kontos, PhD

From the Department of Radiology, University of Pennsylvania, 3700 Hamilton Walk, Richards Bldg, Room D702, Philadelphia, PA 19104 (A.G., L.P., E.A.C., A.D.A.M., E.F.C., D.K.); and the Department of Quantitative Health Sciences, Mayo Clinic, Rochester, Minn (C.G.S., F.F.W., S.J.W., M.R.J., C.M.V.). Received January 26, 2021; revision requested March 16; revision received June 30; accepted July 8. **Address correspondence to** D.K. (e-mail: *Despina.Kontos@pennmedicine.upenn.edu*).

Supported by the Susan G. Komen for the Cure Breast Cancer Foundation (grant PDF17479714), National Cancer Institute of the National Institutes of Health (R01 Research Projects 2R01CA161749-05 and R01CA177150), and a Resource-Related Research Project–Cooperative Agreement (grant 1U24CA189523-01A1).

Conflicts of interest are listed at the end of this article.

See also the editorial by Yaffe in this issue.

Radiology 2021; 301:561–568 • https://doi.org/10.1148/radiol.2021210190 • Content codes: BR CT

Background: While digital breast tomosynthesis (DBT) is rapidly replacing digital mammography (DM) in breast cancer screening, the potential of DBT density measures for breast cancer risk assessment remains largely unexplored.

Purpose: To compare associations of breast density estimates from DBT and DM with breast cancer.

Materials and Methods: This retrospective case-control study used contralateral DM/DBT studies from women with unilateral breast cancer and age- and ethnicity-matched controls (September 19, 2011–January 6, 2015). Volumetric percent density (VPD%) was estimated from DBT using previously validated software. For comparison, the publicly available Laboratory for Individualized Breast Radiodensity Assessment software package, or LIBRA, was used to estimate area-based percent density (APD%) from raw and processed DM images. The commercial Quantra and Volpara software packages were applied to raw DM images to estimate VPD% with use of physics-based models. Density measures were compared by using Spearman correlation coefficients (r), and conditional logistic regression was performed to examine density associations (odds ratios [OR]) with breast cancer, adjusting for age and body mass index.

Results: A total of 132 women diagnosed with breast cancer (mean age ± standard deviation [SD], 60 years ± 11) and 528 controls (mean age, 60 years ± 11) were included. Moderate correlations between DBT and DM density measures (r = 0.32–0.75; all $P < .001$) were observed. Volumetric density estimates calculated from DBT (OR, 2.3 [95% CI: 1.6, 3.4] per SD for VPD%$_{DBT}$) were more strongly associated with breast cancer than DM-derived density for both APD% (OR, 1.3 [95% CI: 0.9, 1.9] [$P < .001$] and 1.7 [95% CI: 1.2, 2.3] [$P = .004$] per SD for LIBRA raw and processed data, respectively) and VPD% (OR, 1.6 [95% CI: 1.1, 2.4] [$P = .01$] and 1.7 [95% CI: 1.2, 2.6] [$P = .04$] per SD for Volpara and Quantra, respectively).

Conclusion: The associations between quantitative breast density estimates and breast cancer risk are stronger for digital breast tomosynthesis compared with digital mammography.

Online supplemental material is available for this article.

Breast cancer risk assessment has become increasingly important in personalized breast cancer screening strategies (1), and numerous studies have consistently validated the strong relationship between increased breast density and breast cancer risk (2–4). The most commonly used breast density assessment method is visual assessment wherein breast density is categorized based on the American College of Radiology Breast Imaging Reporting and Data System (BI-RADS), which is a subjective process (5). Most fully automated methods for breast density assessment, including ImageJ-based research methods (6) and the publicly available Laboratory for Individualized Breast Radiodensity Assessment (LIBRA) software tool (7,8), provide area-based density metrics from two-dimensional (2D) digital mammography (DM) images (8–11). However, DM is rapidly being replaced by digital breast tomosynthesis (DBT), approved by the United States Food and Drug Administration in 2011 (12). In many facilities, DBT technology is also used to reconstruct "synthetic 2D images," which may make conventional DM obsolete (13). Therefore, in view of the rapid clinical conversion to DBT imaging, fully automated methods to measure breast density from DBT are becoming increasingly essential.

In DBT, quasi–three-dimensional breast image volumes are reconstructed from a series of low-dose, 2D raw projection images acquired across a limited angle (14). By providing a quasi–three-dimensional image set, DBT offers the ability to quantify dense breast tissue volumetrically, which in turn may allow for more accurate breast density measures and improved breast cancer risk estimations (15). Attempts have been made by Food and Drug Administration–cleared commercial software vendors, such as

Abbreviations

2D = two-dimensional, APD% = area-based percent density, AUC = area under the receiver operating characteristic curve, BI-RADS = Breast Imaging Reporting and Data System, DA = dense area, DBT = digital breast tomosynthesis, DM = digital mammography, DM-PRO = measures from processed DM views with LIBRA, DM-Q = measures from raw DM views generated by Quantra, DM-RAW = measures from raw DM views with LIBRA, DM-V = measures from raw DM views generated by Volpara, DV = dense volume, LIBRA = Laboratory for Individualized Breast Radiodensity Assessment, OR = odds ratio, SD = standard deviation, VBD = volumetric breast density, VPD% = volumetric percent density

Summary

Volumetric breast density estimates from reconstructed breast tomosynthesis images may have stronger associations with breast cancer than area-based and model-approximated volumetric density measures derived from conventional digital mammography.

Key Results

- Volumetric percent density (VPD%) from digital breast tomosynthesis (DBT) images was associated with breast cancer (odds ratio [OR], 2.3 per standard deviation [SD] of VPD%), after adjusting for standard risk factors.
- DBT-derived VPD% was more strongly associated with breast cancer than area-based percent density from digital mammography (DM) (OR, 1.3 per SD for raw DM and 1.7 for processed DM) and DM-derived VPD% (OR, 1.6 and 1.7 per SD).

Volpara (9) and Hologic (maker of Quantra) (11), to extrapolate volumetric breast density (VBD) from 2D mammographic images with physics-based models incorporating compressed breast thickness. Although such VBD measures have strong associations with breast cancer risk (3,16,17), they are only an approximation of the actual volume of dense tissue, leaving the potential of incorporating fully volumetric DBT-based breast density measures into breast cancer risk assessment largely unexplored.

Using a previously validated software tool for VBD assessment from DBT-reconstructed volumetric data (18), we evaluated the associations between DBT-VBD measures and breast cancer. In addition, we compared our results for DBT-derived breast density estimates with breast cancer associations of *(a)* area-based density metrics extracted from DM images with use of the publicly available LIBRA software package and *(b)* VBD measures extrapolated from DM images using the Volpara and Quantra software packages.

Materials and Methods

Study Design and Data Acquisition

In this institutional review board–approved, Health Insurance Portability and Protection Act–compliant study under a waiver of consent, we retrospectively analyzed a case-control sample of women screened per the dual-modality protocol, DM with DBT (Appendix E1 [online]). This protocol was implemented for all screening examinations at our institution from September 19, 2011, through January 6, 2015, after which DM was replaced by synthetic 2D mammography (37 247 studies from 11 359 individual women).

All women diagnosed with unilateral invasive breast cancer (biopsy- and state registry–confirmed) who also had standard views, as well as both raw (for processing) and processed (for presentation) DM/DBT data available for the screening examination that prompted the cancer diagnosis were included in this study (n = 132). For each patient, we used the images of the unaffected (contralateral) breast at the time of diagnosis, as done in prior related studies (19).

Eligible individuals for the control group were women who had a negative screening examination during the same time period and confirmed negative follow-up at least 1 year later. Controls were matched 4:1 to patients with breast cancer according to age at screening (within 5-year bins), ethnicity, and screening examination date (within 1 year), yielding a total sample of 660 women. For individuals within the control group, we used images from the same side as the breast analyzed for the corresponding cancer case.

Image Acquisition

Clinical risk factor data and DM/DBT images were acquired with Selenia Dimensions units (Hologic). The images from the standard acquisition angles (craniocaudal and mediolateral oblique) or "views" from the DM/DBT screening studies were analyzed. The DM and DBT images used for density calculations were obtained at the same time during a single compression.

Breast Density Evaluation from DBT and DM

VBD evaluation from DBT.—For DBT-derived VBD (VBD_{DBT}), we used a previously validated, automated algorithm that provides VBD metrics, shown to be strongly correlated with VBD measures from MRI scan volumes (18). Briefly, upon segmenting the breast region, the DBT VBD algorithm performs initial segmentation of the dense tissue in DBT projection images, which is then refined in the reconstructed DBT data by radiomic machine learning to identify blurring effects. Summing the dense voxel volumes provides total absolute dense volume (DV), and normalizing DV by the total breast volume gives volumetric percent density (VPD%). In our analysis, we used the DV (DV_{DBT}) and VPD% ($VPD\%_{DBT}$) generated from both DBT views available for each woman.

Area-based density evaluation from DM.—The publicly available LIBRA software (version 1.0.4) (7), previously used in various research studies of breast density (20–23), can calculate area-based density from either raw or processed DM images (8). Briefly, LIBRA partitions the breast region into density clusters of similar gray-level intensity, which are then aggregated into the final dense tissue segmentation. Summing the area of dense pixels provides total absolute dense area (DA), and normalizing DA by the total breast area gives area-based percent density (APD%). We used the DA and APD% estimates obtained from both raw ($DA_{DM\text{-}RAW}$ and $APD\%_{DM\text{-}RAW}$) and processed ($DA_{DM\text{-}PRO}$ and $APD\%_{DM\text{-}PRO}$) DM views available for each woman.

VBD evaluation from DM.—The commercially available Quantra (version 2.1) (11) and Volpara (version 1.5.3, Vol-

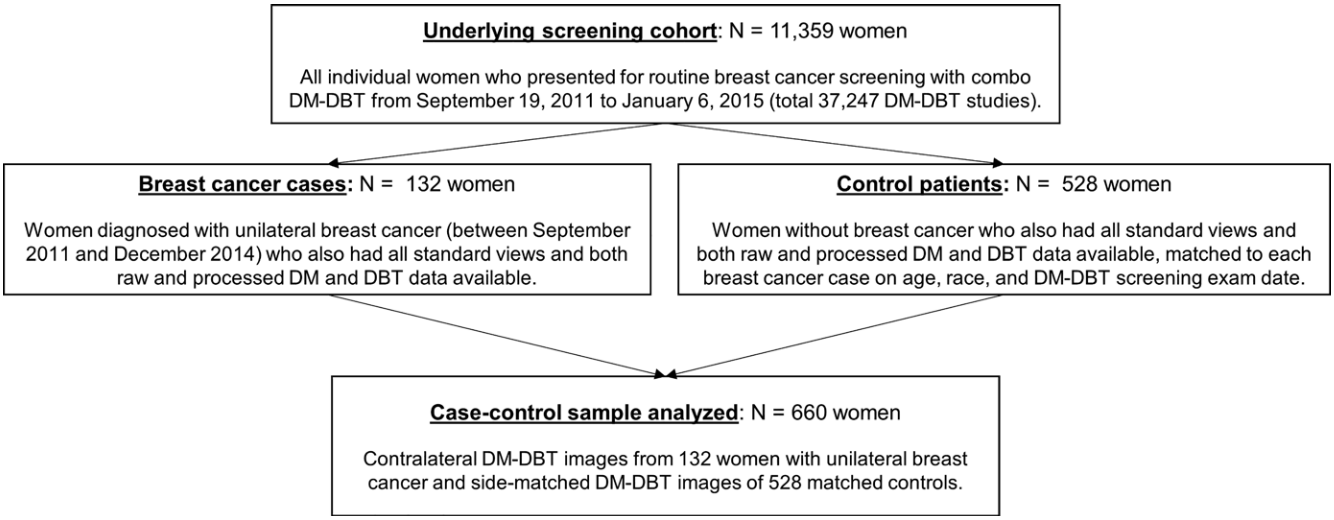

Figure 1: Flowchart shows criteria for case-control selection. DBT = digital breast tomosynthesis, DM = digital mammography.

para Health Technologies) (9) software packages can assess VBD from raw DM images. Using the image pixel intensities, known x-ray attenuations for dense versus fatty tissue, and the Digital Imaging and Communications in Medicine, or DICOM, header values for breast thickness and compression, Quantra and Volpara approximate the thickness of adipose versus fibroglandular tissue within each pixel of the DM image. In both cases, summing the approximations of dense pixel volumes provides DV, and normalizing DV by the total breast volume gives VPD%. We used the DV and VPD% generated by Quantra ($DV_{DM\text{-}Q}$ and $VPD\%_{DM\text{-}Q}$) and Volpara ($DV_{DM\text{-}V}$ and $VPD\%_{DM\text{-}V}$) from both raw DM views available for each woman.

Statistical Analysis

A per-woman value of each density measure was generated by averaging the corresponding density estimates from both breast views (craniocaudal and mediolateral oblique). Spearman correlation coefficients (*r*) were calculated to investigate correlations between DBT and DM density measures. The association between each density measure and breast cancer was evaluated with use of conditional logistic regression (adjusting for age and body mass index) for modeling, and each density measure was log-transformed to account for its skewed distributions. Our sample provided 80% power to detect an odds ratio (OR) as low as 1.3 per 1 standard deviation (SD) in density measure, assuming a type 1 error rate of 0.05.

Results were summarized as ORs and estimates of the area under the receiver operating characteristic curve (AUC) with 95% CIs. To compare non–DBT-derived ORs and AUCs versus the null hypothesis that they were not different from DBT-derived values, 1000 bootstrap samples were chosen at random while maintaining the matched groups, and *P* values were then computed with use of two-sided tests based on comparisons across these 1000 samples. All tests of statistical significance were at the standard α = .05 level. All statistical analyses and plotting were performed in Python 3.7.4.

Table 1: Data Set Characteristics by Case-Control Status

Characteristic	Breast Cancer Group (*n* = 132)	Control Group (*n* = 528)	*P* Value*
Age (y)[†]	60 ± 11	60 ± 11	.84
Body mass index (kg/m^2)[†‡]	30.2 ± 7.5	28.7 ± 7.0	.04
Ethnicity			>.99
White	64 (48)	256 (48)	
Black	62 (47)	248 (47)	
Other or unknown	6 (5)	24 (5)	
Menopausal status			.59
Premenopause	36 (27)	129 (24)	
Postmenopause	95 (72)	393 (74)	
Unknown	1 (0.75)	6 (1.1)	
BI-RADS density category			.11
A	9 (7)	70 (13)	
B	72 (55)	295 (56)	
C	47 (36)	154 (29)	
D	4 (3)	9 (2)	

Note.—Unless otherwise specified, data are numbers of patients, with percentages in parentheses. BI-RADS = Breast Imaging Reporting and Data System.

* *P* values from two-sided Wilcoxon rank-sum tests for continuous covariates and χ^2 tests for categorical covariates.

† Data are means ± standard deviations.

‡ One patient of the 132 with breast cancer (0.8%) and five individuals of the 528 in the control group (0.9%) were missing body mass index information.

Results

Data Set Characteristics

The study data set was composed of 132 women diagnosed with invasive breast cancer (mean age ± SD, 60 years ± 11) and 528 matched control patients (mean age, 60 years ± 11; *P* = .84) (Fig 1). Patients with breast cancer had a higher mean body mass

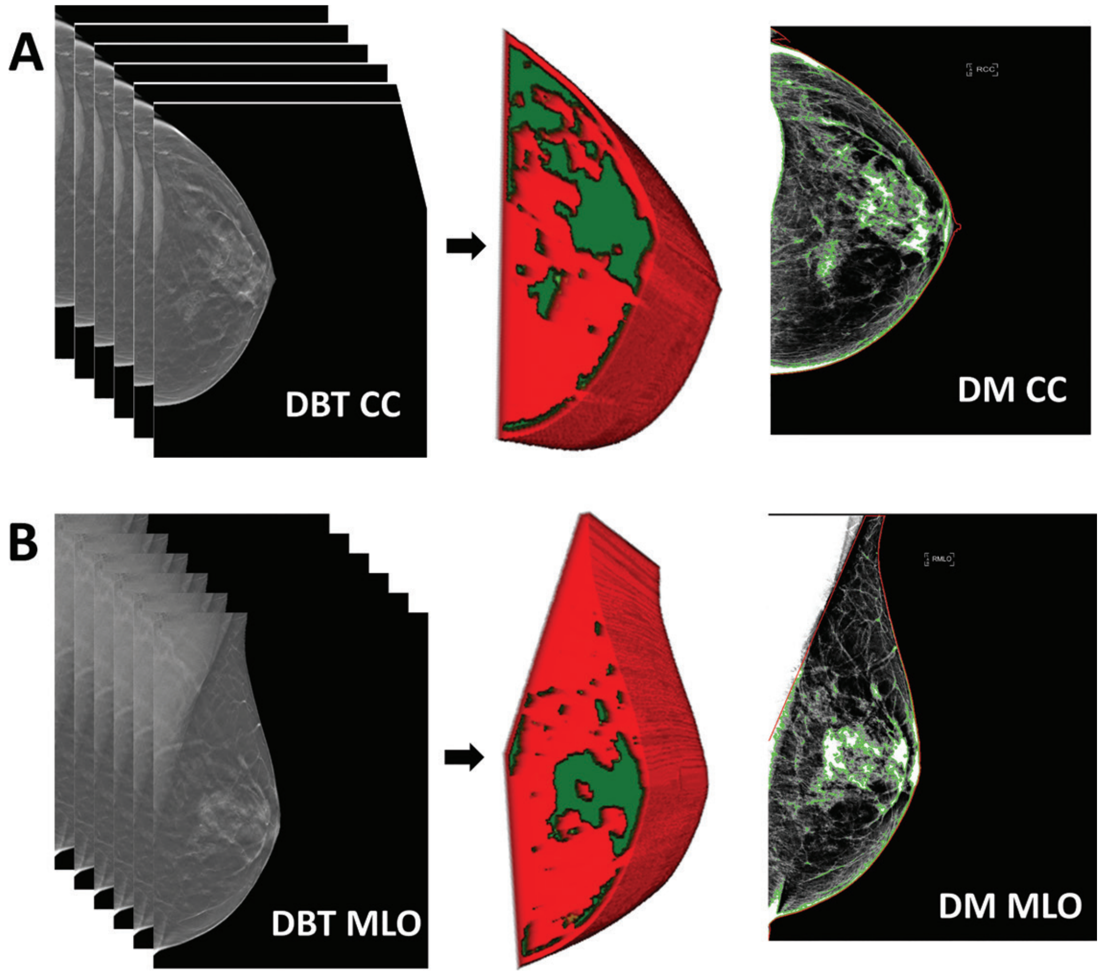

Figure 2: Examples of volumetric breast density evaluation from digital breast tomosynthesis (DBT) and digital mammography (DM) in **(A)** craniocaudal (CC) and **(B)** mediolateral oblique (MLO) breast views, which were obtained in the same woman (aged 56 years, from the control group) at the same time. Volumetric measurements of volumetric percent density of 17.1% and density volume of 71.9 cm^3 were obtained from DBT (where dense-tissue regions of the breast are marked in green). Area-based breast measurements obtained from DM were percent density of 19.2% and density area of 17.2 cm^2.

index compared with individuals in the control group (30.2 kg/m^2 ± 7.5 [SD] vs 28.7 kg/m^2 ± 7.0; P = .04) (Table 1); there were no differences in ethnicity, menopausal status, or BI-RADS density category.

Correlations between DBT and DM Density Measures

We first examined DBT measures with area-based density measures (Fig 2). $VPD\%_{DBT}$ was moderately correlated with $APD\%_{DM\text{-}RAW}$ (r = 0.67, $P < .001$) and $APD\%_{DM\text{-}PRO}$ (r = 0.75, $P < .001$) (Fig 3). DV_{DBT} was weakly correlated with $DA_{DM\text{-}RAW}$ (r = 0.39, $P < .001$) and $DA_{DM\text{-}PRO}$ (r = 0.32, $P < .001$). When volumetric metrics from DBT and DM were compared, $VPD\%_{DBT}$ was moderately correlated with $VPD\%_{DM\text{-}Q}$ (r = 0.61, $P < .001$) and $VPD\%_{DM\text{-}V}$ (r = 0.75, $P < .001$). In addition, DV_{DBT} showed moderate correlations with $DV_{DM\text{-}Q}$ (r = 0.65, $P < .001$) and $DV_{DM\text{-}V}$ (r = 0.62, $P < .001$). All correlations further differed by level of BI-RADS density and breast thickness, with stronger correlations in dense breasts (ie, BI-RADS density C and D) and in lower breast thickness strata (Figs E1, E2 [online]).

Associations of DBT and DM Breast Density Measures with Breast Cancer

Most breast density measures were positively associated with breast cancer (ORs, 1.5–2.6) in conditional logistic regression models that also included age and body mass index (Table 2). In comparisons with area-based models, $VPD\%_{DBT}$ had a stronger association with breast cancer (OR, 2.3 [95% CI: 1.6, 3.4] per SD) than $APD\%_{DM\text{-}RAW}$ (OR, 1.3 [95% CI: 0.9, 1.9] per SD; $P < .001$) and $APD\%_{DM\text{-}PRO}$ (OR, 1.7 [95% CI: 1.2, 2.3] per SD; P = .004). Similar trends were observed for absolute density measures, with DV_{DBT} having a stronger association with breast cancer (OR, 2.3 [95% CI: 1.5, 3.5] per SD) than $DA_{DM\text{-}PRO}$ (OR, 1.5 [95% CI: 1.0, 2.2] per SD; P = .02), but not with $DA_{DM\text{-}RAW}$ (OR, 1.8 [95% CI: 1.2, 2.7] per SD; P = .22). DBT also showed higher discrimination of breast cancer: $VPD\%_{DBT}$ resulted in an AUC of 0.62 (95% CI: 0.57, 0.68), whereas results from $APD\%_{DM\text{-}RAW}$ (AUC, 0.58 [95% CI: 0.52, 0.63]; P = .04) and $APD\%_{DM\text{-}PRO}$ (AUC, 0.60 [95% CI: 0.54, 0.65]; P = .048) were lower.

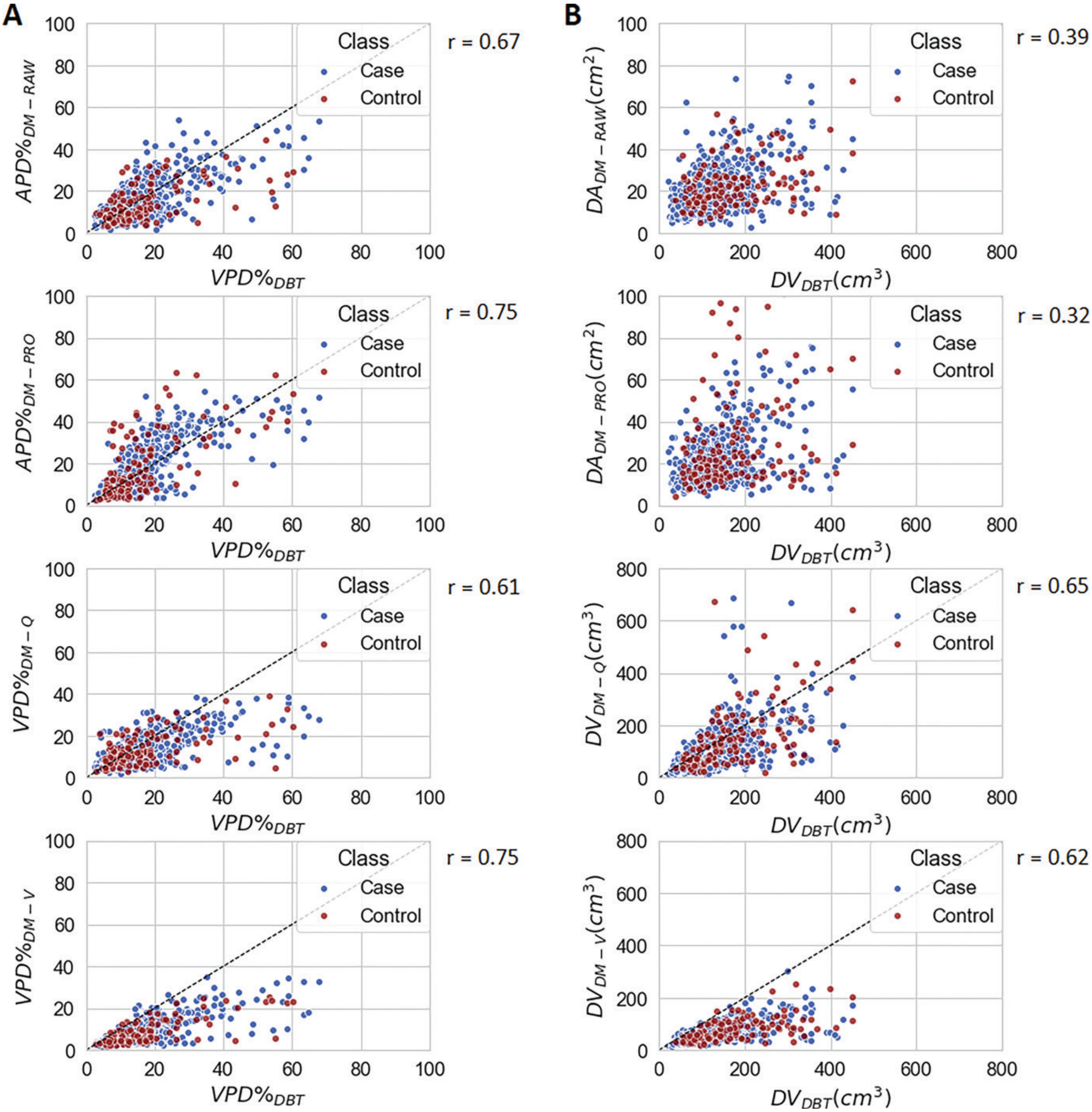

Figure 3: Correlations between digital breast tomosynthesis (DBT) and digital mammography (DM) **(A)** percent and **(B)** absolute breast density measures according to case-control status. Identity line (dashed line) is also shown for reference. APD% = area-based percent density, DA = dense area, DM-PRO = measures from processed DM views with the Laboratory for Individualized Breast Radiodensity Assessment, DM-Q = measures from raw DM views generated by Quantra, DM-RAW = measures from raw DM views with the Laboratory for Individualized Breast Radiodensity Assessment, DM-V = measures from raw DM views generated by Volpara, DV = dense volume, VBD = volumetric breast density, VPD% = volumetric percent density.

$VPD\%_{DBT}$ also had stronger associations with breast cancer (OR, 2.3 [95% CI: 1.6, 3.4] per SD) than did $VPD\%_{DM\text{-}Q}$ (OR, 1.7 [95% CI: 1.2, 2.6]; $P = .04$) and $VPD\%_{DM\text{-}V}$ (OR, 1.6 [95% CI: 1.1, 2.4]; $P = .01$) (Table 2). However, there were no differences between DV_{DBT} measures and DV measures from DM ($DV_{DM\text{-}Q}$ and $DV_{DM\text{-}V}$) measures in their associations with breast cancer ($P > .05$, with ORs of 1.9 and 2.6), and there were no differences among the AUCs of all VBD models ($P > .05$, with AUCs from 0.59 to 0.62) (Table 2).

The AUC of the case-control classification performance based on clinical BI-RADS density assessments on the same data set was 0.58 (95% CI: 0.51, 0.60), which was lower than the performance of all automated DM and DBT density measures (Tables 2, E2 [online]).

Table 2: DBT and DM Breast Density Measures: Distributions according to Case-Control Status and Associations with Breast Cancer

Density Measure	Breast Cancer Group (*n* = 132)	Control Group (*n* = 528)	Odds Ratio	Odds Ratio *P* Value*	AUC	AUC *P* Value*
Area- and volume-based percent density						
$VPD\%_{DBT}$	16.1 ± 12.0	15.4 ± 11.0	2.3 (1.6, 3.4)	Ref	0.62 (0.57, 0.68)	Ref
$APD\%_{DM\text{-}RAW}$	14.0 ± 8.5	14.3 ± 10.0	1.3 (0.9, 1.9)	<.001	0.58 (0.52, 0.63)	.04
$APD\%_{DM\text{-}PRO}$	18.7 ± 15.0	16.3 ± 12.3	1.7 (1.2, 2.3)	.004	0.60 (0.54, 0.65)	.048
$VPD\%_{DM\text{-}Q}$	13.0 ± 7.3	12.1 ± 7.4†	1.7 (1.2, 2.6)	.04	0.59 (0.53, 0.65)	.11
$VPD\%_{DM\text{-}V}$	8.0 ± 5.7	7.9 ± 6.1	1.6 (1.1, 2.4)	.01	0.59 (0.53, 0.64)	.07
Dense volume and dense area						
DV_{DBT} (cm^3)	172.0 ± 90.3	138.9 ± 73.4†	2.3 (1.5, 3.5)	Ref	0.62 (0.57, 0.67)	Ref
$DA_{DM\text{-}RAW}$ (cm^2)	23.5 ± 11.3	20.9 ± 11.5†	1.8 (1.2, 2.7)	.22	0.60 (0.55, 0.65)	.20
$DA_{DM\text{-}PRO}$ (cm^2)	29.4 ± 22.3	22.1 ± 13.4†	1.5 (1.0, 2.2)	.02	0.59 (0.54, 0.64)	.07
$DV_{DM\text{-}Q}$ (cm^3)	151.7 ± 118.2	112.3 ± 83.4†	1.9 (1.4, 2.7)	.15	0.61 (0.55, 0.66)	.27
$DV_{DM\text{-}V}$ (cm^3)	80.3 ± 42.6	64.4 ± 34.8†	2.6 (1.7, 4.0)	.77	0.62 (0.57, 0.68)	.67

Note.—Unless otherwise specified, data are means ± standard deviations. Data in parentheses are 95% CIs. Odds ratios and area under the receiver operating characteristic curve (AUC) values were calculated from logistic regression models adjusted for age and body mass index. Odds ratios are per 1 standard deviation of the log-transformed density measure. APD% = area-based percent density, DA = dense area, DBT = digital breast tomography, DM = digital mammography, DM-PRO = measures from processed DM views with the Laboratory for Individualized Breast Radiodensity Assessment, DM-Q = measures from raw DM views generated by Quantra, DM-RAW = measures from raw DM views with the Laboratory for Individualized Breast Radiodensity Assessment, DM-V = measures from raw DM views generated by Volpara, DV = dense volume, ref = reference measure, VPD% = volume-based percent density.

* *P* values for difference in odds ratio or AUC from the corresponding reference measure.

† Indicates statistically significant difference compared with patients with breast cancer, based on the two-sided Wilcoxon rank-sum test.

Discussion

Our study evaluated the associations of volumetric breast density (VBD) measures estimated from the quasi–three-dimensional data from digital breast tomosynthesis (DBT) with breast cancer risk. Our findings showed that fully automated volumetric estimates of breast density from DBT images were significantly associated with invasive breast cancer at time of mammographic examination, with over twofold risks per standard deviation of volumetric percent density and dense volume, after adjusting for standard risk factors. Comparing results with models using density measures based on digital mammography (DM), area-based density measures from the Laboratory for Individualized Breast Radiodensity Assessment software package, or LIBRA, and VBD measures from the Quantra and Volpara software packages, our DBT-based models showed stronger associations with breast cancer. Furthermore, we showed higher or similar case-control discriminatory capacity for models based on DBT VBD estimates compared with those using density from DM.

The importance of volumetric density estimates in further refining breast cancer risk assessment has been shown in previous studies (10,20), where breast cancer associations were highest for Volpara VPD% compared with semi- and fully automated APD% measures. However, both studies evaluated model-approximated VPD% derived from raw DM, not from DBT volumes, as we did here.

Our study also showed only moderate correlations between DBT and DM density measures, which also varied with density and breast thickness categories. Such differences may be due to a combination of factors. Overall, with the removal of anatomic noise (such as the superimposed densities from skin and subcutaneous tissue in DBT), DBT breast density estimates are expected to be lower than those derived from DM (24). However, breast density, when volumetrically assessed from multiple reconstructed DBT sections in dense breasts, may be estimated at higher values than those from DM (25), where denser tissue is summed. At the same time, more anatomic noise is introduced into an image as breast thickness increases. Furthermore, vendor-specific image processing and reconstruction algorithms applied to generate the reconstructed sections may make certain tissue arrangements more discernible in the reconstructed sections, which in turn may lead to more accurate identification of dense versus fatty tissue. Finally, an additional factor affecting correlation of VBD density estimates from DBT compared with DM is that methods estimating VBD with DM rely on physics-based models; however, as with all models, there are assumptions made that may not be appropriate for all women. Although it is uncertain which effects tend to dominate in density correlations between DM and DBT as well as which density estimate is closer to the "true" value of breast density, these findings show the need for a careful refinement of density-based risk calculations as imaging shifts from DM to DBT screening (26).

A strength of our study was access to paired DM/DBT images obtained at the same time under a single compression, avoiding possible variability or bias in the results due to differences in breast compression, position, device, or even technician effects between DM and DBT. Another major strength was data from a racially diverse population (48% White, 47% Black), which allows generalizability of our results to larger portions of the United States or even global populations. Finally, in comparing with several established (both research and commercial) tools for density estimation from DM, our study offers wide applicability and enhanced translation to clinical application, strengthening the potential impact of our findings compared with other studies on breast density and risk.

Certain limitations should also be noted. We performed our study using contralateral mammograms of patients with invasive breast cancer, rather than prior screening images of women in whom breast cancer was later detected. This is a common first-step approach (19), based on the premise that a woman's breasts—both affected and contralateral—share inherent breast tissue properties that predispose her to a certain risk of developing breast cancer. Additionally, due to the relatively short period of DM/DBT screening at our institution (before implementation of synthetic 2D mammography/DBT) and the need for raw DM/DBT data (which is not routinely stored), the size of our study data set, driven by the number of patients with breast cancer, was only moderate, and access to prior negative DM/DBT screening studies was limited. In future studies, we aim to validate our findings in larger cohorts, using also screening images from years prior to a cancer diagnosis, which will pave the way to the first public release of our VBD_{DBT} algorithm. Future evaluation of DBT-derived density will also include potential integration with density measures from synthetic 2D mammography, as this imaging technique is rapidly replacing DM in DBT imaging (27). Furthermore, we will explore potential integration with breast parenchymal complexity features, which are complementary to breast density and can be generated by emerging radiomic and deep learning methods (28,29), toward further improving breast cancer risk assessment with DBT.

In conclusion, fully automated, quantitative, volumetric estimates of breast density from digital breast tomosynthesis (DBT) reconstructed data results in stronger associations with breast cancer than either area-based density estimates from conventional, planar digital mammography (DM) or volumetric density estimates from DM. Our results further extend the advantages of the new standard of breast cancer screening, DBT, showing a path to improved quantitative breast density calculation, which may result in improved breast cancer risk assessment.

Author contributions: Guarantors of integrity of entire study, E.F.C., D.K.; study concepts/study design or data acquisition or data analysis/interpretation, all authors; manuscript drafting or manuscript revision for important intellectual content, all authors; approval of final version of submitted manuscript, all authors; agrees to ensure any questions related to the work are appropriately resolved, all authors; literature research, A.G., E.F.C., D.K.; clinical studies, C.M.V., E.F.C.; statistical analysis, A.G., C.G.S., E.A.C., S.J.W., M.R.J., A.D.A.M., C.M.V., D.K.; and manuscript editing, A.G., C.G.S., E.A.C., S.J.W., A.D.A.M., C.M.V., E.F.C., D.K.

Disclosures of Conflicts of Interest: **A.G.** disclosed no relevant relationships. **L.P.** disclosed no relevant relationships. **C.G.S.** disclosed no relevant relationships. **E.A.C.** disclosed no relevant relationships. **F.F.W.** disclosed no relevant relationships. **S.J.W.** disclosed no relevant relationships. **M.R.J.** disclosed no relevant relationships. **A.D.A.M.** disclosed compensation as a scientific board member of Real Time Tomography; received compensation for expert testimony on patent infringement lawsuits from Williams and Connolly and from Jones Day Arnold & Porter; received or will receive grants from the National Institutes of Health, Department of Defense, Susan G. Komen Breast Cancer Foundation, and Burroughs Wellcome Fund; has patents pending; has stocks or stock options in Real Time Tomography and Daimroc; received funds to cover travel and meeting expenses from KTH Sweden. **C.M.V.** institution received grant from GRAIL for liquid biopsy marker research. **E.F.C.** disclosed compensation as a member of the iCAD advisory panel; institution received or will receive grants from Hologic, OM1, and iCAD; received speaker fees from AuntMinnie.com. **D.K.** institution received or will receive a research grant from Hologic.

References

1. Shieh Y, Eklund M, Madlensky L, et al. Breast cancer screening in the precision medicine era: risk-based screening in a population-based trial. J Natl Cancer Inst 2017;109(5):djw290.
2. McCormack VA, dos Santos Silva I. Breast density and parenchymal patterns as markers of breast cancer risk: a meta-analysis. Cancer Epidemiol Biomarkers Prev 2006;15(6):1159–1169.
3. Brandt KR, Scott CG, Miglioretti DL, et al. Automated volumetric breast density measures: differential change between breasts in women with and without breast cancer. Breast Cancer Res 2019;21(1):118.
4. Bond-Smith D, Stone J. Methodological challenges and updated findings from a meta-analysis of the association between mammographic density and breast cancer. Cancer Epidemiol Biomarkers Prev 2019;28(1):22–31.
5. American College of Radiology. Breast Imaging Reporting and Data System (BI-RADS) Atlas. Reston, Va: American College of Radiology, 2013.
6. Li J, Szekely L, Eriksson L, et al. High-throughput mammographic-density measurement: a tool for risk prediction of breast cancer. Breast Cancer Res 2012;14(4):R114.
7. Laboratory for Individualized Breast Radiodensity Assessment (LIBRA). https://www.cbica.upenn.edu/sbia/software/LIBRA/. Accessed December 1, 2020.
8. Keller BM, Nathan DL, Wang Y, et al. Estimation of breast percent density in raw and processed full field digital mammography images via adaptive fuzzy c-means clustering and support vector machine segmentation. Med Phys 2012;39(8):4903–4917.
9. Highnam R, Brady M, Yaffe MJ, Karssemeijer N, Harvey J. Robust breast composition measurement - Volpara™. In: Digital Mammography (IWDM). Berlin, Germany: Springer, 2010; 342–349.
10. Eng A, Gallant Z, Shepherd J, et al. Digital mammographic density and breast cancer risk: a case-control study of six alternative density assessment methods. Breast Cancer Res 2014;16(5):439.
11. Hartman K, Highnam R, Warren R, Jackson V, eds. Volumetric Assessment of Breast Tissue Composition from FFDM Images. In: Digital Mammography (IWDM). Berlin, Germany: Springer, 2008.
12. U.S. Food and Drug Administration. Mammography Quality Standards Act and Program - 2020 Scorecard Statistics. https://www.fda.gov/radiation-emitting-products/mqsa-insights/2020-scorecard-statistics. Accessed December 1, 2020.
13. Bernardi D, Macaskill P, Pellegrini M, et al. Breast cancer screening with tomosynthesis (3D mammography) with acquired or synthetic 2D mammography compared with 2D mammography alone (STORM-2): a population-based prospective study. Lancet Oncol 2016;17(8):1105–1113.
14. Sechopoulos I. A review of breast tomosynthesis. Part I. The image acquisition process. Med Phys 2013;40(1):014301.
15. Chong A, Weinstein SP, McDonald ES, Conant EF. Digital breast tomosynthesis: concepts and clinical practice. Radiology 2019;292(1):1–14.
16. Vachon CM, Brandt KR, Ghosh K, et al. Mammographic breast density as a general marker of breast cancer risk. Cancer Epidemiol Biomarkers Prev 2007;16(1):43–49.
17. Brandt KR, Scott CG, Ma L, et al. Comparison of clinical and automated breast density measurements: implications for risk prediction and supplemental screening. Radiology 2016;279(3):710–719.
18. Pertuz S, McDonald ES, Weinstein SP, Conant EF, Kontos D. Fully automated quantitative estimation of volumetric breast density from digital breast tomosynthesis images: preliminary results and comparison with digital mammography and MR imaging. Radiology 2016;279(1):65–74.
19. Gastounioti A, Conant EF, Kontos D. Beyond breast density: a review on the advancing role of parenchymal texture analysis in breast cancer risk assessment. Breast Cancer Res 2016;18(1):91.
20. Gastounioti A, Kasi CD, Scott CG, et al. Evaluation of LIBRA software for fully automated mammographic density assessment in breast cancer risk prediction. Radiology 2020;296(1):24–31.

21. Nguyen TL, Choi Y-H, Aung YK, et al. Breast cancer risk associations with digital mammographic density by pixel brightness threshold and mammographic system. Radiology 2018;286(2):433–442.
22. Busana MC, Eng A, Denholm R, et al. Impact of type of full-field digital image on mammographic density assessment and breast cancer risk estimation: a case-control study. Breast Cancer Res 2016;18(1):96.
23. Ambrale SS, Rounds T, Sussman BL, et al. The influence of inflammation on mammographic breast density in women at increased risk of breast cancer. J Clin Oncol 2015;33(15_Suppl):1566.
24. Förnvik D, Förnvik H, Fieselmann A, Lång K, Sartor H. Comparison between software volumetric breast density estimates in breast tomosynthesis and digital mammography images in a large public screening cohort. Eur Radiol 2019;29(1):330–336.
25. Machida Y, Saita A, Namba H, Fukuma E. Automated volumetric breast density estimation out of digital breast tomosynthesis data: feasibility study of a new software version. Springerplus 2016;5(1):780.
26. Gastounioti A, McCarthy AM, Pantalone L, Synnestvedt M, Kontos D, Conant EF. Effect of mammographic screening modality on breast density assessment: digital mammography versus digital breast tomosynthesis. Radiology 2019;291(2):320–327.
27. Conant EF, Keller BM, Pantalone L, Gastounioti A, McDonald ES, Kontos D. Agreement between breast percentage density estimations from standard-dose versus synthetic digital mammograms: results from a large screening cohort using automated measures. Radiology 2017;283(3):673–680.
28. Kontos D, Winham SJ, Oustimov A, et al. Radiomic phenotypes of mammographic parenchymal complexity: toward augmenting breast density in breast cancer risk assessment. Radiology 2019;290(1):41–49.
29. Dembrower K, Liu Y, Azizpour H, et al. Comparison of a deep learning risk score and standard mammographic density score for breast cancer risk prediction. Radiology 2020;294(2):265–272.